Published in final edited form as:
Cytokine. 2015 February ; 71(2): 302–311. doi:10.1016/j.cyto.2014.11.010.

Structural and agonist properties of XCL2, the other member of the C-chemokine subfamily

Jamie C. Fox[a], **Takashi Nakayama**[b], **Robert C. Tyler**[a], **Tara Sander**[c], **Osamu Yoshie**[d], and **Brian F. Volkman**[a,*]

[a]Department of Biochemistry, Medical College of Wisconsin, Milwaukee, WI 53226, USA

[b]Division of Chemotherapy, Kinki University Faculty of Pharmacy, Higashi-osaka 577-8502, Japan

[c]Department of Pediatric Pathology, Medical College of Wisconsin, Milwaukee, WI 53226, USA

[d]Kinki University Faculty of Medicine, Osaka-Sayama, Osaka 589-851, Japan

Abstract

Known for its unusual metamorphic native state structure, XCL1 has been the focus of most efforts to elucidate the structural, functional, and physiological properties of chemokines in the C subfamily. By comparison, its closely related paralog XCL2 remains virtually uncharacterized. Based on the importance of the chemokine N-terminus in receptor activation, it was hypothesized that two amino acid differences in XCL2 would alter its agonist activity relative to XCL1 for their shared receptor XCR1. This present study reveals several properties of XCL2 that were unexamined until now. Structurally, XCL1 and XCL2 are very similar, exchanging between the monomeric chemokine fold and an unrelated dimeric state under physiological NaCl and temperature conditions. Ca^{2+} flux, chemotaxis, and heparin binding assays showed that the monomer form of XCL2 is responsible for G protein-coupled receptor activation while the dimeric form is important for GAG binding. Despite their high structural similarity, XCL2 displays a slightly higher affinity for heparin than XCL1. Because their *in vitro* functional profiles are virtually identical, distinct physiological roles for XCL1 and XCL2 are probably encoded at the level of expression.

Keywords

XCL2; XCL1; Lymphotactin; chemotaxis; Ca^{2+} flux; heparin

*To whom correspondence should be addressed: Brian F. Volkman, Department of Biochemistry, Medical College of Wisconsin, 8701 Watertown Plank Road, Milwaukee, WI 53226, USA. Tel: +1 (414) 955-8400; Fax: (414) 955-6510; bvolkman@mcw.edu.

1. INTRODUCTION

The chemokine signaling network is composed of approximately 50 secreted ligands and 20 G-protein coupled receptors (GPCRs). Research has shown that this complex system is involved in a variety of physiological processes including mediation of cellular migration during immune responses [1, 2], maintenance of homeostatic mechanisms [3], progression of inflammatory and autoimmune diseases, and cancer metastasis [4]. Chemokines are divided into four major sub-families, CC, CXC, CX_3C, and C, based on the positions of conserved cysteine residues near the amino terminus. Despite sharing a high level of tertiary structure homology [5], chemokines are relatively specific for the receptors they bind and the effects they mediate. Based on our knowledge of chemokine structure-function relationships and their physiological roles, the chemokine system has become a target for development of therapeutic agents in cancer and many other diseases. The C chemokine sub-family is composed of two members, XCL1 (also known as lymphotactin, Ltn, ATAC, SCYC-1, or SCM1-α), and XCL2 (SCM1-β, SCYC-2) [6]. The cognate receptor for these chemokines is XCR1 [7]. In near-physiological solution conditions (phosphate-buffered saline at 37 °C), XCL1 exhibits a dynamic conformational equilibrium between structurally unrelated monomer and dimer states [8, 9], a unique characteristic that distinguishes XCL1 from all other chemokines. The monomeric form (also known as Ltn10), displaying the canonical chemokine fold, binds and activates XCR1. The dimer conformation (Ltn40) binds with high affinity to extracellular matrix glycosaminoglycans (GAGs) [10–12] and lacks XCR1 agonist activity. GAG binding is essential for establishment of chemokine gradients that provide directional cues for migrating cells. Based on our previous structural studies, we produced XCL1 variants designed to bias the Ltn10-Ltn40 equilibrium and isolate either conformational state. The CC3 variant contains a second disulfide bond that locks XCL1 in the monomer form and prevents conversion to the Ltn40 state. The W55D variant swaps out a hydrophobic tryptophan residue with a negatively charged aspartic acid, destabilizing the hydrophobic core formed in the monomer and promoting Ltn40 dimer formation [11, 12].

XCL1 is an inflammatory chemokine that is mainly secreted by activated $CD8^+$ T cells [13–17] and its biological function is the subject of renewed scrutiny. The earliest reports described XCL1 as a mediator of T cell and NK cell chemotaxis [14–17]. However, recent studies suggest a highly specialized role of the XCL1-XCR1 signaling axis in the mediation of interactions between antigen-presenting dendritic cells and T-cells [18–20], induction of $CD8^+$ effector T-cell responses [21], and formation of self-tolerance mechanisms through the development of T_{reg} cells within the thymus [22, 23].

Discovered simultaneously by three different groups in mid-1990s [15–17, 24], XCL1 has become the main focus of C-chemokine studies and little is known about the structural and functional properties of its closely related paralog, XCL2. Yoshida and colleagues identified *XCL2* through screens of a human whole blood genomic library. *XCL1* and *XCL2* mapped to chromosome 1, and RT-PCR analysis revealed XCL1 and XCL2 transcripts in both mitogen stimulated and non-stimulated cells [25]. XCL1 and XCL2 are constitutively expressed by unstimulated natural killer (NK) cells and to a lesser extent by inactive $CD8^+$ T cells [26]. Upon stimulation with IL-2, NK cells showed a marked increase in XCL1 expression while

XCL2 expression continued to be expressed at constitutive levels [26, 27]. On the other hand, activation of T cells resulted in a dramatic increase in XCL1 and XCL2 expression in $CD8^+$ T cells [26, 28]. Activated $CD4^+$ T cells demonstrated increased amounts of XCL2, but not XCL1 [28]. XCL1 and XCL2 are also induced by cancer and bacterial pathogens. In cancers such as epithelial ovarian and hepatocellular carcinoma, increased XCL2 expression correlates with cancer progression [29, 30]. In patients with indolent chronic lymphocytic leukemia, XCL1 and XCL2 are expressed by $CD4^+$ and $CD8^+$ T cells at significantly higher levels than in healthy subjects or multiple myeloma patients [31]. In a separate study, addition of a tuberculosis antigen, Wag31 induced the expression of XCL2 but not XCL1 in macrophages [32]. Taken together, the published studies indicate that expression of XCL1 and XCL2 are regulated separately and function independently *in vivo*. However the structural properties and *in vitro* activity of the XCL2 protein have not yet been characterized.

Chemokines interact with their cognate receptors through a two-site mechanism. At the first site, the N-terminus of the GPCR binds to an epitope on the body of the chemokine. Insertion of the N-terminus of the chemokine into a cavity in the transmembrane domain of the GPCR (site 2) induces a conformational change within the receptor and heterotrimeric G-protein activation [33]. The human XCL2 and XCL1 amino acid sequences differ at only two positions near the N-terminus: D7 and K8 in XCL1 are replaced by H7 and R8 in XCL2 [25]. We speculated that the non-conservative aspartic acid to histidine substitution in XCL2 might alter its activity as an XCR1 agonist relative to XCL1.

In the present study, we used bioinformatic analysis to confirm the presence of *XCL2* in multiple species, and then produced recombinant human XCL2 protein to enable the first structural and functional comparisons with XCL1. Like the metamorphic XCL1 protein, XCL2 interconverts between two distinct conformational states. *In vitro* measurements of XCR1 activation and cellular chemotaxis revealed no significant functional differences between the two proteins, however XCL2 exhibited slightly higher GAG binding affinity.

2. EXPERIMENTAL PRODCEURES

2.1 Genomic database searches and sequence alignments

XCL1 and XCL2 nucleotide and amino acid sequences for various species were identified through searches of the National Center for Biotechnology Information (NCBI) Gene database (http://www.ncbi.nlm.nih.gov/gene). XCL1 searches revealed sequences for the following species: human (Gene ID: 6375), bonobo (Gene ID: 100978961) chimpanzee (Gene ID: 469572), baboon (Gene ID: 101004038), squirrel monkey (Gene ID: 101052132), galago (Gene ID: 100959305), goat (Gene ID: 102190981), alpaca (Gene ID: 102526821), camel (Gene ID: 102507143), walrus (Gene ID: 101383122), seal (Gene ID: 102743023), ferret (Gene ID: 101672337), manatee (Gene ID: 101357913), fox (Gene ID: 102888482), brown bat (Gene ID: 102423013), Brandt's bat (Gene ID: 102246603), hedgehog (Gene ID: 101650865), mole (Gene ID: 102820708), shrew (Gene ID: 102855080), cotton rat (Gene ID: 71845256), Norway rat (Gene ID: 171371), chinchilla (Gene ID: 102017550), ground squirrel (Gene ID: 101970885), prairie vole (102000194), hamster (Gene ID: 101830061),

degu (Gene ID: 101566538), chicken (Gene ID: 395914), soft-shelled turtle (Gene ID: 102457828), alligator (Gene ID: 102382163), and painted turtle (Gene ID: 101938916).

Additional sequences for XCL1 were identified using Ensembl genome database (http://www.ensembl.org/index.html). These species included: gorilla (Gene ID: ENSG00000143185), orangutan (Gene ID: ENSPPYG00000000539), gibbon (Gene ID: ENSNLEG00000014923), macaque (Gene ID: ENSMMUG00000010085), bushbaby (Gene ID: ENSOGAG00000011103), marmoset (Gene ID: ENSCJAG00000010361), lemur (Gene ID: ENSMICG00000007410), pig (Gene ID: ENSSSCG00000020892), bovine (Gene ID: ENSBTAG00000009943), sheep (Gene ID: ENSOARG00000009100), cat (Gene ID: ENSFCAG00000029190), dog (gene ID: ENSCAFG00000029542), dolphin (Gene ID: ENSTTRG00000021414), horse (gene ID: ENSECAG00000013872), rabbit (Gene ID: ENSOCUG00000012952), pika (Gene ID: ENSOPRG00000006314), elephant (Gene ID: ENSLAFG00000017780), megabat (Gene ID: ENSPVAG00000009459), microbat (Gene ID: ENSMLUG00000011950), armadillo (Gene ID: ENSDNOG00000042103), opossum (Gene ID: ENSMODG00000002933), Tasmanian devil (Gene ID: ENSSHAG00000018950), mouse (Gene ID: ENSMUSG00000026573), guinea pig (Gene ID: ENSCPOG00000023218), zebra finch (Gene ID: ENSTGUG00000013433), Duck (Gene ID: ENSAPLG00000016429), flycatcher (Gene ID: ENSFALG00000005712), and turkey (Gene ID: ENSMGAG00000014351).

XCL2 sequences were found upon searching the NCBI Gene database mentioned above. These species included: human (Gene ID: 6846), chimpanzee (Gene ID: 735318), and degu (101572785). The following XCL2 sequences were found on the Ensembl database: orangutan (Gene ID: ENSPPYG00000000538), gibbon (Gene ID: ENSNLEG00000005765), macaque (Gene ID: ENSMMUG00000013779), pig (Gene ID: ENSSSCG00000006298), bovine (Gene ID: ENSBTAG00000009938), dolphin (Gene ID: ENSTTRG00000021400), sheep (Gene ID: ENSOARG00000009179), opossum (Gene ID: ENSMODG00000027516), Tasmanian devil (Gene ID: ENSSHAG00000004166), and guinea pig (Gene ID: ENSCPOG00000012457). These database searches were completed on or before April 10th, 2014. Sequences were aligned with Jalview Multiple Alignment Editor software using the clustal default settings (BLOSUM62 matrix, open gap penalty setting = 10) [34, 35].

2.2 Purification of recombinant XCL1 and XCL2 proteins

Recombinant XCL1 WT and CC3 variants were expressed in BL21 (DE3) *E. coli* transfected with pET28a expression vectors containing the sequence for His-SUMO-XCL1. Cultures were grown in terrific broth or minimal M9 media containing 50 μg/ml kanamycin to an optical density at 600 nm = 0.6 at 37 °C. Protein expression was induced with 1mM isopropyl-β-D-thiogalactopyranoside (IPTG). The cultures were then incubated for 5 h at 37 °C. After incubation, the bacteria were pelleted by centrifugation. Pellets were resuspended in 50 mM sodium phosphate (pH 8.0), 300 mM NaCl, 10 mM imidazole, 0.1% (v/v) 2-mercaptethanol, 1 mM phenylmethylsufonyl fluoride (PMSF), and lysed by three passages through a French pressure cell. The cell lysates were centrifuged to pellet the inclusion body. The soluble fraction was collected and set aside. The inclusion body was resuspsended

in 50 mM sodium phosphate (pH 8.0), 6 M guanidine HCl, 300 mM NaCl, 10 mM imidazole, and 0.1% (v/v) 2-mercaptethanol, and centrifuged. The supernatant was collected and combined with the soluble fraction collected earlier. The mixture was incubated with columns containing Ni^{2+}- NTA resin (Qiagen) for 30 min at RT. The columns were rinsed with 50 mM sodium phosphate (pH 8.0), 6 M guanidine HCl, 300 mM NaCl, 10 mM imidazole, and 0.1% (v/v) 2-mercaptethanol. His-tagged proteins were eluted from the resin with 100 mM sodium acetate (pH 4.5), 6 M guanidine HCl, 300 mM NaCl, and 10 mM imidazole. Eluted protein was then refolded by infinite dilution in 20 mM Tris (pH 8.0), 200 mM NaCl, 10 mM cysteine, and 0.5 mM cystine, and incubated at room temperature overnight while stirring. After incubation, the protein solution was then concentrated to < 20 mL using an Amicon stirred-cell concentrator. The protein solution was diluted in order to reduce the NaCl concentration to 25 mM. ULP1 protease was added to the protein solution to cleave off the His-SUMO fusion from XCL1. The cleavage reaction was incubated at 30 °C overnight. Cation exchange chromatography was used to purify the His-SUMO tag from XCL1. Upon loading the SP-sepharose Fast Flow (Amersham) resin with the cleavage reaction, the column was washed with 20 mM Tris (pH 8.0), and 25 mM NaCl. The protein was eluted with 20 mM Tris (pH 8.0) and 5 M NaCl. As a final step, the protein was purified by reverse phase HPLC. Fractions containing XCL1 were collected and the molecular weight was confirmed by MALDI-TOF mass spectrometry. The QuikChange Site-directed mutagenesis kit (Stratagene) was used to mutate the XCL1 expression vector to XCL2. Recombinant XCL2 was purified as described above.

2.3 HSQC screening and K_{eq} measurements

A series of NMR heteronuclear quantum coherence experiments (HSQC) were conducted, as previously described [9, 11, 12], to determine whether XCL2 is able to interconvert between the chemokine monomer and alternative dimer states observed for XCL1. Briefly, temperature and NaCl concentrations were varied to shift the equilibrium and access the different conformational states, as described in the results sections. The data was processed using NMRPipe [36]. CARA (Computer Aided Resonance Assignment) [37] software was used to measure peak volumes. These peak volumes were used to calculate equilibrium constants and are represented as K_{eq} ± SEM for XCL1 and XCL2.

2.4. 2D ^{1}H-^{15}N Heteronuclear ZZ Exchange NMR and calculation of rate constants

1 mM protein samples were prepared by diluting protein stock into 20 mM phosphate (pH 6.0) and 10% D_2O. Exchange spectra were collected on a Bruker 600 MHz NMR spectrometer at the following mixing times: 0.05, 0.15, 0.2, 0.25, 0.3, 0.35, 0.4, 0.5, 0.6, 0.75, and 0.9 s. The data was processed using NMRPipe, as described above. The volumes of the auto and cross peaks for each mixing time were calculated using XEASY software [38]. Peak volumes were plotted as a function of mixing time, and the data was fit to calculate forward (k_{fwd}) and reverse (k_{rev}) using MatLab® software as previously described [39].

2.5. Calculation of $\Delta G_{unfolding}$ from urea-induced unfolding measurements

Protein unfolding was measured from fluorescence measurements of WT XCL1 or XCL2 protein at 5 μM in 20 mM phosphate, pH 6.0, containing from 0 to 9 M urea. Tryptophan

fluorescence was monitored at 332 nm using a PTI fluorometer (Birmingham, NJ) and Microsoft Excel was used to analyze fluorescence data and calculate $\Delta G_{unfolding}$ values using linear extrapolation as previously described [40].

2.6. Ca^{2+} flux assay

The Ca^{2+} flux assays were carried out using stably transfected XCR1- expressing HEK 293 cells generously provided by Dr. Joseph Hedrick (Schering-Plough Research Institute) [41]. Cultured cells grown to ~ 90% confluency were lifted from culture plates with Enzyme-Free Cell Dissociation Buffer (Gibco) and resuspended in assay buffer (1x HBSS, 20 mM HEPES (pH 7.4), and 0.1% BSA) [42]. In a 96-well format, cells were plated at 2.0 x 10^5 cells/well in 100 μL. The cells were incubated with 100 μL of FLIPR Calcium 4 Assay Dye (Molecular Devices, Sunnyvale, CA) for 1 h at 37 °C and 5% CO_2. A Flexstation 3 (Molecular Devices) was used to treat the cells with various concentrations of purified proteins and monitor Ca^{2+} flux. EC_{50} values were determined using Pro Fit 6.1.11 software. Assays were conducted in replicates of six and EC_{50} values are represented as mean ± S.D.

2.7. Chemotaxis assay

Chemotaxis assays were carried out using murine L1.2 cells stably expressing human XCR1 [7]. In brief, 2.0 x10^5 cells were suspended in 25 μL of assay media (phenol red free RPMI 1640, 0.5% BSA, and 10mM HEPES (pH 7.4)) and added to the upper chambers of a transwell assay plate. XCL1 and XCL2 proteins were diluted to various concentrations in 30 μL of the same medium and added to the lower chambers. The plates were incubated at 37 °C and 5% CO_2 for 1.5 h. After incubations, cells that migrated into lower wells were lysed with 0.1% Triton X-100 and measured by PicoGreen double-stranded DNA quantitation reagent (Molecular Probes, Eugene, OR). Assays were conducted in duplicate and the numbers of cells in the lower wells were expressed as a percentage of input cells. Results are shown as mean ± SEM from three separate experiments.

2.8. Heparin and S-sepharose Binding Assay

Electrostatic and GAG binding were assessed for XCL1 and XCL2 proteins using cation exhange SP-sepharose and heparin-sepharose chromatography, respectively [43, 44]. Approximately 200 μg of purified proteins were individually loaded onto 1 mL HiTrap SP-Sepharose HP and 1 mL HiTrap Heparin HP columns (GE Healthcare, Sweden) attached to a Shimadzu Prominence HPLC and subjected to a 0 – 1M NaCl gradient in 20 mM phosphate (pH 6.0 and pH 7.0) buffer. Protein elution was monitored by recording the absorbance at 280 nm.

3. RESULTS

3.1. XCL2 is present in a limited range of species

In order to address the question of whether *XCL2* exists as a distinct gene in organisms other than humans, NCBI and Ensembl databases were searched for *XCL1* and *XCL2* gene distribution. *XCL1* was found in a variety of animal genomes including birds, rodents, and apes. An alignment of the respective amino acid sequences is found in Figure 1A.

Unlike *XCL1*, *XCL2* is found in a smaller sample of organisms including, human, chimpanzee, orangutan, gibbon, macaque, pig, bovine, sheep, dolphin, opossum, Tasmanian devil, guinea pig, and degu. There is no evidence of a second XCL gene in mouse and rat genomes. An alignment of the XCL1 and XCL2 amino acid sequences (Fig 1B) illustrates their high similarity. As noted previously [25], the human proteins differ at only two sequence positions, ^{7}DK^{8} and ^{7}HR^{8} in XCL1 and XCL2, respectively. Interestingly, the $D7_{(XCL1)}$ to $H7_{(XCL2)}$ change that occurs in the human sequences is a unique non-conservative mutation that eliminates a negatively charged side chain. With the exception of the chimpanzee, Tasmanian devil, and opossum sequences, which contains a non-conservative $D7_{(XCL1)}$ to $N7_{(XCL2)}$ mutation or basic residue mutations, respectively, an acidic residue remains in the seventh position in all other XCL2 proteins.

XCL1 is located on the forward strand of their respective chromosomes in human, chimpanzee, and orangutan, guinea pig, Tasmanian devil, pig, macaque, degu while *XCL2* is found on the reverse strand. Bovine, sheep, opossum, and gibbon *XCL1* and *XCL2* genes are both located on the forward strands, while the two dolphin genes are located on the reverse strand of their chromosome.

Certain chemokines, particularly from the CXC subfamily, are found in reptiles, amphibian, and fish species [45, 46]. With the exception of a “lymphotactin-like” sequence in *Xenopus tropicalis* (XP_002939969), there is little evidence for *XCL1/XCL2* sequences in these species. It has been speculated that *XCL1* has undergone a recent gene duplication event, giving rise to a highly homologous gene known as *XCL2* [25]. XCL2 expression in human cells has been reported [25, 27], but it is unknown whether XCL2 is expressed as a functional protein in other species.

3.2. XCL2 interconverts between two distinct structures

We showed previously that XCL1 exists in a highly unique conformational equilibrium between two unrelated states (Fig 2A). A chemokine-like monomer (Ltn10) is prevalent at conditions of high salt and low temperature (150 mM NaCl, 10 °C) (Fig 2B), while a novel dimeric (Ltn40) structure is stabilized at low salt and higher temperature (0 mM NaCl, 40 °C) (Fig 2D). In near physiological solution conditions (phosphate buffered saline, 37 °C) the two conformations are equally abundant (Fig 2C). By changing the temperature and salt, it is possible to shift the equilibrium and visualize NMR peak patterns that are unique and representative of each native state structure [11]. The corresponding heteronuclear single quantum coherence (HSQC) spectra for XCL2 are seen in figure 2E–G. The similarity of their 2D NMR profiles suggests that, like XCL1, XCL2 interconverts between the Ltn10 monomer and Ltn40 dimer states. Plots of chemical shift differences between the XCL1 and XCL2 spectra collected at 10 °C, 150 mM NaCl (Fig 2H) and 40 °C, 0 mM NaCl (Fig 2I) show that significant chemical shift differences are localized to the vicinity of amino acid variations at sequence positions 7 and 8. Taken together this data illustrates the conservation of structural features between XCL1 and XCL2, and reveals XCL2 as the newest example of a metamorphic protein.

3.3. The monomeric form of XCL2 is important for activation of XCR1

Chemokine binding and receptor activation typically initiates a downstream signaling cascade that leads to release of Ca^{2+} from internal stores, cell polarization, and chemotactic migration. Due to the metamorphic nature of XCL2, we sought to determine the functional significance of this conformational exchange on the ability of XCL2 to activate XCR1. To assess the agonist activity of XCL2, a series of experiments were conducted to test for Ca^{2+} flux and chemotactic responses of XCR1-expressing cells treated with WT, locked monomer (CC3), and preferential dimer (W55D) constructs of XCL1 and XCL2. A concentration response experiment measuring Ca^{2+} flux in XCR1-transfected HEK 293 cells (Fig 3A) revealed comparable EC_{50} values for the monomeric CC3 forms of XCL1 and XCL2 (EC_{50} ~ 15 nM). Chemotactic responses of murine L1.2 cells treated with CC3 versions of XCL1 and XCL2 yielded a typical biphasic response, seen for most other chemokines [47], with maximal cellular migration observed at 1 nM protein concentration (Fig 3D). The potencies of WT XCL2 matched XCL1 in Ca^{2+} flux (EC_{50} ~ 50 nM; Fig 3 B) and chemotaxis measurements (maximal response at 10 nM; Fig 3E). Unlike WT and CC3 variants, XCL1 and XCL2 W55D did not demonstrate measureable Ca^{2+} flux within the tested concentration range (Fig 3C). The W55D variants were not further examined for chemotaxis response. In each case the WT protein showed reduced potency relative to the CC3 variant, consistent with the monomeric Ltn10 conformation acting as the XCR1 agonist for both XCL1 and XCL2.

3.4. XCL2 dimer binds to heparin with slightly higher affinity than XCL1 dimer

In addition to binding their cognate GPCRs, chemokines also bind to glycosaminoglycans (GAGs) in the extracellular matrix, establishing concentration gradients that are essential for providing directional cues for cellular migration. Most chemokines are highly basic proteins, with isoelectric points (pI) ~ 9. However, chemokine-GAG affinity is not simply a function of electrostatic attraction, but rather a combination of both specific affinity and electrostatic contributions. For example, chemokines such as CCL3 and CCL4 demonstrate heparin binding despite having acidic pI values [43, 44, 48]. To characterize their non-specific electrostatic and specific GAG binding, purified XCL1 and XCL2 proteins were subjected to cation exchange SP-sepharose and heparin sepharose chromatography, respectively. As a measure of the specific affinity of each protein-heparin interaction, we computed the differences in salt concentrations required to elute each protein from cation exchange and heparin columns (ΔΔ[NaCl]; Table 1) [43]. To assess the impact of the Asp7 to His7 substitution in XCL2, experiments were conducted at pH 6.0 and 7.0.

We observed measurable differences in the cation exchange SP-sepharose elution profiles of XCL1 and XCL2 proteins. WT and CC3 XCL1 proteins eluted at < 500 mM NaCl, while WT and CC3 XCL2 eluted at > 500 mM NaCl (Fig 4C,E & Table 1). The W55D variants of both XCL1 and XCL2 demonstrated the highest retention. This difference between the XCL1 and XCL2 proteins at pH 6.0 was expected due to the protonation of His7. XCL1 and XCL2 peaks remain separated at pH 7.0, but the separation is slightly decreased from pH 6.0 (Fig 4D,F).

Elution profiles from the heparin chromatography experiments showed a distinct separation between W55D and CC3 proteins at pH 6.0 and pH 7.0 (Fig. 4A,B,E,F & Table 1). Both WT and W55D XCL proteins displayed similar affinities to heparin indicating a heparin-induced shift in WT equilibrium toward dimerization. Evidence of the monomer conformation is observed in elution profiles for WT proteins and appear as a small peak shoulder eluting at similar NaCl concentrations as the CC3 locked monomers (Fig 4A,B). Compared to all proteins tested, XCL2 WT and W55D displayed the highest affinity for heparin at pH 6.0 (Fig 4A,E & Table 1). As in the cation exchange experiments, a pH dependent retention shift is observed between XCL1 and XCL2 species. This data demonstrates three important aspects of XCL2 – GAG interactions: 1) the Ltn40 conformation of XCL2 is responsible for high affinity heparin-binding, 2) XCL2 has a slightly higher affinity for heparin than XCL1, and 3) protonation of His7 may contribute to an increase in XCL2 heparin affinity relative to XCL1.

3.5 Thermodynamic and kinetic parameters of XCL2

Upon observing that XCL2 had a slight increase in heparin affinity, we began to probe the kinetic and thermodynamic properties of WT XCL2 to see if there were any observable changes in the stability and conformational equilibrium of this protein. A series of urea-induced unfolding experiments were conducted to test the stability of the Ltn10 state of both XCL1 and XCL2. Values of $\Delta G_{unfolding}$ were calculated under conditions that tested for effects of NaCl addition. There were no discernable differences between $\Delta G_{unfolding}$ values collected for XCL1 and XCL2. These values were 2.3 ± 0.1 and 2.1 ± 0.1 kcal/mol in the absence of NaCl and 2.8 ± 0.1 and 2.6 ± 0.1 kcal/mol in the presence of 150 mM NaCl, for XCL1 and XCL2, respectively. NaCl is known to stabilize the Ltn10 form [9]

To further analyze the equilibrium process of XCL2, we conducted a series of NMR experiments to determine the equilibrium constants (K_{eq}), and forward (k_{fwd}) and reverse rate (k_{rev}) constants. Table 2 represents data that was collected at 20 mM phosphate (pH 6.0), 25 °C, and ± 150 mM NaCl. k_{fwd} and k_{rev} values were collected from $^{1}H - ^{15}N$ heteronuclear ZZ exchange NMR experiments. The k_{fwd}/k_{rev} values are calculated from the measured rate constants and represent the equilibrium constant. In addition to the calculated K_{eq} values, K_{eq} (last column) was measured using a separate NMR technique. These parameters for XCL1 and XCL2 are highly similar, suggesting that the interconversion process between the Ltn10 and Ltn40 forms is conserved. The values determined here for XCL1 correspond well with previously reported rate constants [9, 12].

4. Discussion & Conclusions

The physiological role of XCL1 is currently being reexamined. Initially thought to function as a broad lymphocyte chemoattractant, recent reports suggest a highly specific role for XCL1 in mediating dendritic cell - T cell interactions [21–23]. In the active efforts to elucidate the biological function of XCL1, XCL2 is typically ignored. As a foundation for future investigations of the role of XCL2 in the immune system, this study provides a detailed *in vitro* description of its structural and functional properties.

While most aspects of these closely related proteins are extremely similar, XCL2 binds with slightly higher affinity to heparin than XCL1. This increased affinity is most prevalent at pH < 7. Currently it is unknown if this increase in heparin/GAG binding is physiologically relevant, however immunological responses are often accompanied by local acidosis at sites of inflammation. The pH in these micro-environments can drop from ~ 7.4 to ~ 6.5 [49]. These shifts in pH are responsible for regulating the activity of effectors such as heparanases [50], influencing the production of chemokines such as CXCL8 [51] and CCL2 [52], and leading to the progression of diseases such as cancer metastasis [53] and inflammatory bowel disease [54]. It is possible that the activity of XCL2 may be influenced by inflammatory pH changes.

Chemokines are subjected to regulation at the level of expression as well as modification of activity at the protein level. XCL1 and XCL2 are under the control of separate promoters on chromosome 1 [25]. A previous study examined the upstream promoter region extending to 0.7-kb preceding both XCL1 and XCL2 genes. They discovered that this region was 97% identical and showed that expression is controlled by a family of transcription factors known as Nuclear Factor of Activated T cell (NFATs) [55]. The NFAT family consists of five members, and certain family members appear to be constitutively expressed in the nuclei of specific cell types [55], while other members are regulated by Ca^{2+} signaling [56]. It is possible that XCL1 and XCL2 are regulated by differences in NFAT levels within distinct cell types. Alternatively, distant upstream promoter and regulatory elements may be responsible for controlling XCL1 and XCL2 expression.

Chemokines are also subjected to various post-translational modifications (PTMs) such as N-terminal truncation [57], and citrullination [58]. In addition, XCL1 is one of the few chemokines reported to be glycosylated *in vivo* [13]. The C-terminus of XCL1 contains a mucin-like domain, harboring eight serine and threonine residues that are sites of O-linked glycosylation [13, 59, 60]. However, the physiological relevance of this modification is not well understood. It is possible that XCL1 and XCL2 are subjected to a wide variety of PTMs.

As described previously, homo-dimerization of XCL1 and XCL2 is important for facilitating high affinity heparin binding. However, it is likely that XCL1 and XCL2 may form heterodimer complexes *in vivo*, which may slightly alter heparin-binding affinity. There are many *in vivo* events that may lead to functional differences between XCL1 and XCL2. However, these events were not examined in our *in vitro* - recombinant protein based system.

It still remains a mystery as to why only a small subset of species has two copies of an XCL gene. It has been speculated that XCL2 arose from a recent gene duplication event [25]. Upon examination of the amino acid sequence, it appears that the XCL1 and XCL2 sequences in human, chimpanzee, orangutan, gibbon, and macaque are more closely related while those for Guinea pig, Tasmanian devil, sheep, dolphin, and bovine seemed to display greater differences (Fig 1B). If gene duplication is responsible for the formation of XCL2, it is possible that separate duplication events occurred in primate versus the non-primate lineages as a result of differential exposure to environmental pathogens. The theoretical

reasons for duplication of genes are controversial. Theories range from duplication events acting as major mechanisms of evolution [61], to a genomic response of an organism to fulfill various requirements for dosage compensation [62]. A more comprehensive phylogenetic analysis may provide interesting insight into the history of XCL1 and origin of XCL2.

In order to fully understand the role of XCL2, *in vivo* studies are needed to test for expression patterns and tissue distributions of XCL1 and XCL2 under certain immune stimuli. As mentioned previously, expression differences occur in response to lymphocyte activation and disease progression [26–32]. Due to their extreme similarity, *in vivo* studies pose challenges of designing primers or antibodies that are specific for the detection of one or the other protein but will provide valuable information about this chemokine family and its role in the immune system.

Acknowledgments

funding (NIH grants AI013325 and AI058072); we thank Evgenii Kovrigin for assistance with MATLAB data analysis.

References

1. Charo IF, Ransohoff RM. The many roles of chemokines and chemokine receptors in inflammation. N Engl J Med. 2006; 354(6):610–621. [PubMed: 16467548]
2. Luster AD. Chemokines--chemotactic cytokines that mediate inflammation. N Engl J Med. 1998; 338(7):436–445. [PubMed: 9459648]
3. Le Y, Zhou Y, Iribarren P, Wang J. Chemokines and chemokine receptors: their manifold roles in homeostasis and disease. Cell Mol Immunol. 2004; 1(2):95–104. [PubMed: 16212895]
4. Murphy PM. Chemokines and the molecular basis of cancer metastasis. N Engl J Med. 2001; 345(11):833–835. [PubMed: 11556308]
5. Fernandez EJ, Lolis E. Structure, function, and inhibition of chemokines. Annu Rev Pharmacol Toxicol. 2002; 42:469–499. [PubMed: 11807180]
6. Zlotnik A, Yoshie O. Chemokines: a new classification system and their role in immunity. Immunity. 2000; 12(2):121–127. [PubMed: 10714678]
7. Yoshida T, Imai T, Kakizaki M, Nishimura M, Takagi S, Yoshie O. Identification of single C motif-1/lymphotactin receptor XCR1. J Biol Chem. 1998; 273(26):16551–16554. [PubMed: 9632725]
8. Kuloglu ES, McCaslin DR, Kitabwalla M, Pauza CD, Markley JL, Volkman BF. Monomeric solution structure of the prototypical 'C' chemokine lymphotactin. Biochemistry. 2001; 40(42): 12486–12496. [PubMed: 11601972]
9. Kuloglu ES, McCaslin DR, Markley JL, Volkman BF. Structural rearrangement of human lymphotactin, a C chemokine, under physiological solution conditions. J Biol Chem. 2002; 277(20): 17863–17870. [PubMed: 11889129]
10. Peterson FC, Elgin ES, Nelson TJ, Zhang F, Hoeger TJ, Linhardt RJ, Volkman BF. Identification and characterization of a glycosaminoglycan recognition element of the C chemokine lymphotactin. J Biol Chem. 2004; 279(13):12598–12604. [PubMed: 14707146]
11. Tuinstra RL, Peterson FC, Elgin ES, Pelzek AJ, Volkman BF. An engineered second disulfide bond restricts lymphotactin/XCL1 to a chemokine-like conformation with XCR1 agonist activity. Biochemistry. 2007; 46(10):2564–2573. [PubMed: 17302442]
12. Tuinstra RL, Peterson FC, Kutlesa S, Elgin ES, Kron MA, Volkman BF. Interconversion between two unrelated protein folds in the lymphotactin native state. Proc Natl Acad Sci U S A. 2008; 105(13):5057–5062. [PubMed: 18364395]

13. Dorner B, Muller S, Entschladen F, Schroder JM, Franke P, Kraft R, Friedl P, Clark-Lewis I, Kroczek RA. Purification, structural analysis, and function of natural ATAC, a cytokine secreted by CD8(+) T cells. J Biol Chem. 1997; 272(13):8817–8823. [PubMed: 9079718]
14. Giancarlo B, Silvano S, Albert Z, Mantovani A, Allavena P. Migratory response of human natural killer cells to lymphotactin. Eur J Immunol. 1996; 26(12):3238–3241. [PubMed: 8977329]
15. Kelner GS, Kennedy J, Bacon KB, Kleyensteuber S, Largaespada DA, Jenkins NA, Copeland NG, Bazan JF, Moore KW, Schall TJ, et al. Lymphotactin: a cytokine that represents a new class of chemokine. Science. 1994; 266(5189):1395–1399. [PubMed: 7973732]
16. Kennedy J, Kelner GS, Kleyensteuber S, Schall TJ, Weiss MC, Yssel H, Schneider PV, Cocks BG, Bacon KB, Zlotnik A. Molecular cloning and functional characterization of human lymphotactin. J Immunol. 1995; 155(1):203–209. [PubMed: 7602097]
17. Muller S, Dorner B, Korthauer U, Mages HW, D'Apuzzo M, Senger G, Kroczek RA. Cloning of ATAC, an activation-induced, chemokine-related molecule exclusively expressed in CD8+ T lymphocytes. Eur J Immunol. 1995; 25(6):1744–1748. [PubMed: 7615002]
18. Bachem A, Guttler S, Hartung E, Ebstein F, Schaefer M, Tannert A, Salama A, Movassaghi K, Opitz C, Mages HW, et al. Superior antigen cross-presentation and XCR1 expression define human CD11c+CD141+ cells as homologues of mouse CD8+ dendritic cells. J Exp Med. 2010; 207(6):1273–1281. [PubMed: 20479115]
19. Crozat K, Guiton R, Contreras V, Feuillet V, Dutertre CA, Ventre E, Vu Manh TP, Baranek T, Storset AK, Marvel J, et al. The XC chemokine receptor 1 is a conserved selective marker of mammalian cells homologous to mouse CD8alpha+ dendritic cells. J Exp Med. 2010; 207(6): 1283–1292. [PubMed: 20479118]
20. Crozat K, Tamoutounour S, Manh TP, Fossum E, Luche H, Ardouin L, Guilliams M, Azukizawa H, Bogen B, Malissen B, et al. Cutting edge: expression of XCR1 defines mouse lymphoid-tissue resident and migratory dendritic cells of the CD8alpha+ type. J Immunol. 2011; 187(9):4411–4415. [PubMed: 21948982]
21. Dorner BG, Dorner MB, Zhou X, Opitz C, Mora A, Guttler S, Hutloff A, Mages HW, Ranke K, Schaefer M, et al. Selective expression of the chemokine receptor XCR1 on cross-presenting dendritic cells determines cooperation with CD8+ T cells. Immunity. 2009; 31(5):823–833. [PubMed: 19913446]
22. Lei Y, Ripen AM, Ishimaru N, Ohigashi I, Nagasawa T, Jeker LT, Bosl MR, Hollander GA, Hayashi Y, de Malefyt RW, et al. Aire-dependent production of XCL1 mediates medullary accumulation of thymic dendritic cells and contributes to regulatory T cell development. J Exp Med. 2011; 208(2):383–394. [PubMed: 21300913]
23. Lei Y, Takahama Y. XCL1 and XCR1 in the immune system. Microbes Infect. 2011
24. Yoshida T, Imai T, Kakizaki M, Nishimura M, Yoshie O. Molecular cloning of a novel C or gamma type chemokine, SCM-1. FEBS Lett. 1995; 360(2):155–159. [PubMed: 7875320]
25. Yoshida T, Imai T, Takagi S, Nishimura M, Ishikawa I, Yaoi T, Yoshie O. Structure and expression of two highly related genes encoding SCM-1/human lymphotactin. FEBS Lett. 1996; 395(1):82–88. [PubMed: 8849694]
26. Yamazaki C, Miyamoto R, Hoshino K, Fukuda Y, Sasaki I, Saito M, Ishiguchi H, Yano T, Sugiyama T, Hemmi H, et al. Conservation of a chemokine system, XCR1 and its ligand, XCL1, between human and mice. Biochem Biophys Res Commun. 2010; 397(4):756–761. [PubMed: 20541533]
27. Hennemann B, Tam YK, Tonn T, Klingemann HG. Expression of SCM-1alpha/lymphotactin and SCM-1beta in natural killer cells is upregulated by IL-2 and IL-12. DNA Cell Biol. 1999; 18(7): 565–571. [PubMed: 10433555]
28. Wang M, Windgassen D, Papoutsakis ET. Comparative analysis of transcriptional profiling of CD3+, CD4+ and CD8+ T cells identifies novel immune response players in T-cell activation. BMC Genomics. 2008; 9:225. [PubMed: 18485203]
29. Zimmerman JW, Pennison MJ, Brezovich I, Yi N, Yang CT, Ramaker R, Absher D, Myers RM, Kuster N, Costa FP, et al. Cancer cell proliferation is inhibited by specific modulation frequencies. Br J Cancer. 2012; 106(2):307–313. [PubMed: 22134506]

30. Kim M, Rooper L, Xie J, Rayahin J, Burdette JE, Kajdacsy-Balla AA, Barbolina MV. The lymphotactin receptor is expressed in epithelial ovarian carcinoma and contributes to cell migration and proliferation. Molecular cancer research: MCR. 2012; 10(11):1419–1429. [PubMed: 22964431]
31. Kiaii S, Kokhaei P, Mozaffari F, Rossmann E, Pak F, Moshfegh A, Palma M, Hansson L, Mashayekhi K, Hojjat-Farsangi M, et al. T cells from indolent CLL patients prevent apoptosis of leukemic B cells in vitro and have altered gene expression profile. Cancer Immunol Immunother. 2013; 62(1):51–63. [PubMed: 22736254]
32. Cao W, Tang S, Yuan H, Wang H, Zhao X, Lu H. Mycobacterium tuberculosis antigen Wag31 induces expression of C-chemokine XCL2 in macrophages. Curr Microbiol. 2008; 57(3):189–194. [PubMed: 18618175]
33. Crump MP, Gong JH, Loetscher P, Rajarathnam K, Amara A, Arenzana-Seisdedos F, Virelizier JL, Baggiolini M, Sykes BD, Clark-Lewis I. Solution structure and basis for functional activity of stromal cell-derived factor-1; dissociation of CXCR4 activation from binding and inhibition of HIV-1. Embo J. 1997; 16(23):6996–7007. [PubMed: 9384579]
34. Clamp M, Cuff J, Searle SM, Barton GJ. The Jalview Java alignment editor. Bioinformatics. 2004; 20(3):426–427. [PubMed: 14960472]
35. Waterhouse AM, Procter JB, Martin DM, Clamp M, Barton GJ. Jalview Version 2--a multiple sequence alignment editor and analysis workbench. Bioinformatics. 2009; 25(9):1189–1191. [PubMed: 19151095]
36. Delaglio F, Grzesiek S, Vuister GW, Zhu G, Pfeifer J, Bax A. NMRPipe: a multidimensional spectral processing system based on UNIX pipes. J Biomol NMR. 1995; 6(3):277–293. [PubMed: 8520220]
37. Computer-aided resonance assignment (CARA). Available from: http://www.nmr.ch
38. Bartels C, Xia TH, Billeter M, Gunter P, Wuthrich K. The program XEASY for computer-spoorted NMR spectral analysis of biological macromolecules. Journal of Biomoleculear NMR. 1995; 6(1): 1–10.
39. Tyler RC, Wieting JC, Peterson FC, Volkman BF. Electrostatic optimization of the conformational energy landscape in a metamorphic protein. Biochemistry. 2012; 51(45):9067–9075. [PubMed: 23102260]
40. Shirley BA. Urea and guanidine hydrochloride denaturation curves. Methods Mol Biol. 1995; 40:177–190. [PubMed: 7633522]
41. Shan L, Qiao X, Oldham E, Catron D, Kaminski H, Lundell D, Zlotnik A, Gustafson E, Hedrick JA. Identification of viral macrophage inflammatory protein (vMIP)-II as a ligand for GPR5/XCR1. Biochem Biophys Res Commun. 2000; 268(3):938–941. [PubMed: 10679309]
42. Keller RLJ. Computer aided resonance assignment tutorial: Cantina. 2004
43. Hamel DJ, Sielaff I, Proudfoot AE, Handel TM. Chapter 4. Interactions of chemokines with glycosaminoglycans. Methods in Enzymology. 2009; 461:71–102. [PubMed: 19480915]
44. Handel TM, Johnson Z, Crown SE, Lau EK, Proudfoot AE. Regulation of protein function by glycosaminoglycans--as exemplified by chemokines. Annu Rev Biochem. 2005; 74:385–410. [PubMed: 15952892]
45. Baoprasertkul P, He C, Peatman E, Zhang S, Li P, Liu Z. Constitutive expression of three novel catfish CXC chemokines: homeostatic chemokines in teleost fish. Mol Immunol. 2005; 42(11): 1355–1366. [PubMed: 15950731]
46. Huising MO, Stet RJ, Kruiswijk CP, Savelkoul HF, Lidy Verburg-van Kemenade BM. Molecular evolution of CXC chemokines: extant CXC chemokines originate from the CNS. Trends Immunol. 2003; 24(6):307–313. [PubMed: 12810106]
47. Calabrese EJ. Cell migration/chemotaxis: biphasic dose responses. Crit Rev Toxicol. 2001; 31(4–5):615–624. [PubMed: 11504186]
48. Proudfoot AE, Handel TM, Johnson Z, Lau EK, LiWang P, Clark-Lewis I, Borlat F, Wells TN, Kosco-Vilbois MH. Glycosaminoglycan binding and oligomerization are essential for the in vivo activity of certain chemokines. Proc Natl Acad Sci U S A. 2003; 100(4):1885–1890. [PubMed: 12571364]

49. Menkin V, Warner CR. Studies on Inflammation: XIII. Carbohydrate Metabolism, Local Acidosis, and the Cytological Picture in Inflammation. Am J Pathol. 1937; 13(1):25–44. 21. [PubMed: 19970311]
50. Ihrcke NS, Parker W, Reissner KJ, Platt JL. Regulation of platelet heparanase during inflammation: role of pH and proteinases. J Cell Physiol. 1998; 175(3):255–267. [PubMed: 9572470]
51. Xu L, Fidler IJ. Acidic pH-induced elevation in interleukin 8 expression by human ovarian carcinoma cells. Cancer Res. 2000; 60(16):4610–4616. [PubMed: 10969814]
52. Ogata R, Hiramatsu N, Hayakawa K, Nakajima S, Yao J, Kobayashi T, Kitamura M. Impairment of MCP-1 expression in mesothelial cells exposed to peritoneal dialysis fluid by osmotic stress and acidic stress. Perit Dial Int. 2011; 31(1):80–89. [PubMed: 20448242]
53. Rofstad EK, Mathiesen B, Kindem K, Galappathi K. Acidic extracellular pH promotes experimental metastasis of human melanoma cells in athymic nude mice. Cancer Res. 2006; 66(13):6699–6707. [PubMed: 16818644]
54. Nugent SG, Kumar D, Rampton DS, Evans DF. Intestinal luminal pH in inflammatory bowel disease: possible determinants and implications for therapy with aminosalicylates and other drugs. Gut. 2001; 48(4):571–577. [PubMed: 11247905]
55. Yoshida T, Ishikawa I, Ono Y, Imai T, Suzuki R, Yoshie O. An activation-responsive element in single C motif-1/lymphotactin promoter is a site of constitutive and inducible DNA-protein interactions involving nuclear factor of activated T cell. J Immunol. 1999; 163(6):3295–3303. [PubMed: 10477599]
56. Macian F. NFAT proteins: key regulators of T-cell development and function. Nat Rev Immunol. 2005; 5(6):472–484. [PubMed: 15928679]
57. Lambeir AM, Durinx C, Proost P, Van Damme J, Scharpe S, De Meester I. Kinetic study of the processing by dipeptidyl-peptidase IV/CD26 of neuropeptides involved in pancreatic insulin secretion. FEBS Lett. 2001; 507(3):327–330. [PubMed: 11696365]
58. Loos T, Mortier A, Gouwy M, Ronsse I, Put W, Lenaerts JP, Van Damme J, Proost P. Citrullination of CXCL10 and CXCL11 by peptidylarginine deiminase: a naturally occurring posttranslational modification of chemokines and new dimension of immunoregulation. Blood. 2008; 112(7):2648–2656. [PubMed: 18645041]
59. Marcaurelle LA, Mizoue LS, Wilken J, Oldham L, Kent SB, Handel TM, Bertozzi CR. Chemical synthesis of lymphotactin: a glycosylated chemokine with a C-terminal mucin-like domain. Chemistry. 2001; 7(5):1129–1132. [PubMed: 11303872]
60. Dong C, Chua A, Ganguly B, Krensky AM, Clayberger C. Glycosylated recombinant human XCL1/lymphotactin exhibits enhanced biologic activity. J Immunol Methods. 2005; 302(1–2): 136–144. [PubMed: 15992811]
61. Ohno S. Gene duplication and the uniqueness of vertebrate genomes circa 1970–1999. Semin Cell Dev Biol. 1999; 10(5):517–522. [PubMed: 10597635]
62. Hughes T, Ekman D, Ardawatia H, Elofsson A, Liberles DA. Evaluating dosage compensation as a cause of duplicate gene retention in Paramecium tetraurelia. Genome Biol. 2007; 8(5):213. [PubMed: 17521457]

Highlights

- Structural and agonist properties of human XCL2 were examined *in vitro*.
- XCL2 is limited to a small subset of organisms based on bioinformatics analysis.
- XCL2 is structurally similar to XCL1, displaying metamorphic interconversion.
- The monomeric form of XCL2 activates XCR1 and has a similar potency to XCL1.
- XCL2 dimer displays a slightly higher heparin binding affinity than XCL1.

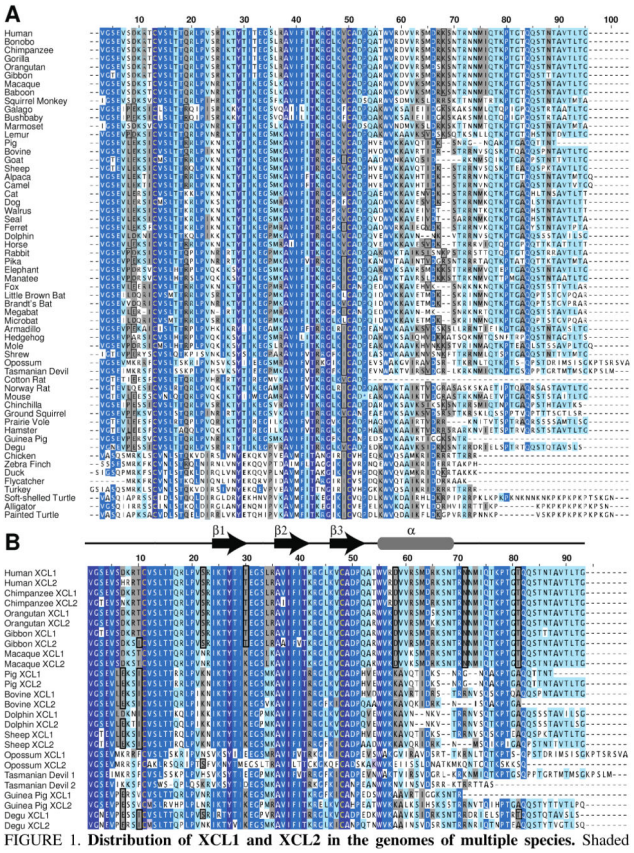

FIGURE 1. **Distribution of XCL1 and XCL2 in the genomes of multiple species.** Shaded

FIGURE 1. Distribution of XCL1 and XCL2 in the genomes of multiple species

Shaded residues share a percent identity with the consensus sequence: dark blue with white text = 100 %, medium blue with white text = > 80 %, cyan with black text = > 50 %, gray with black text = > 25 %, and non-shaded = < 25 %. The cysteine residues are highlighted in dark blue with yellow text. A. Amino acid sequence alignment illustrating the distribution and homology of XCL1 within various species. B. Sequence alignment of species containing XCL1 and XCL2. A schematic of the secondary structure, based on structural studies of the monomeric form of human XCL1, is located above the alignment (β = beta-sheet, α = alpha helix).

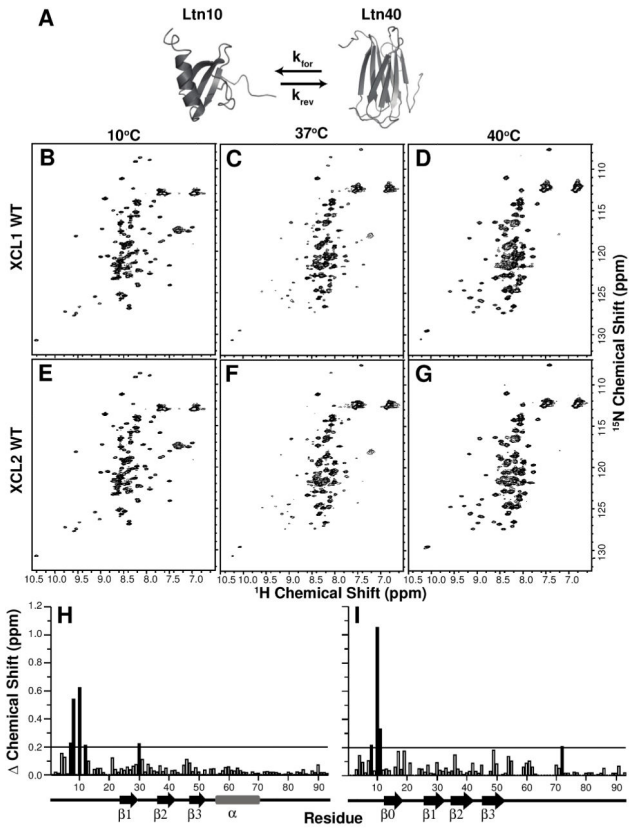

FIGURE 2. HSQC analysis of the native conformational states of WT XCL1 and WT XCL2

A) Schematic of XCL1 equilibrium between dual native states. XCL1 and XCL2 spectra collected at: (B,E) 10 °C, 150 mM NaCl; (C,F) 37 °C, 150 mM NaCl; or (D,G) 40 °C, 0 mM NaCl. Plots of chemical shift differences between XCL1 and XCL2 spectra at 10 °C, 150 mM NaCl (H), and 40 °C, 0 mM NaCl (I). The bars denote the following chemical shift differences: black ≥ 0.2, and open < 2.0 ppm. A schematic of the secondary structure, based on structural studies of human XCL1, is located below the graphs in H & I (β = beta-sheet, α = alpha helix).

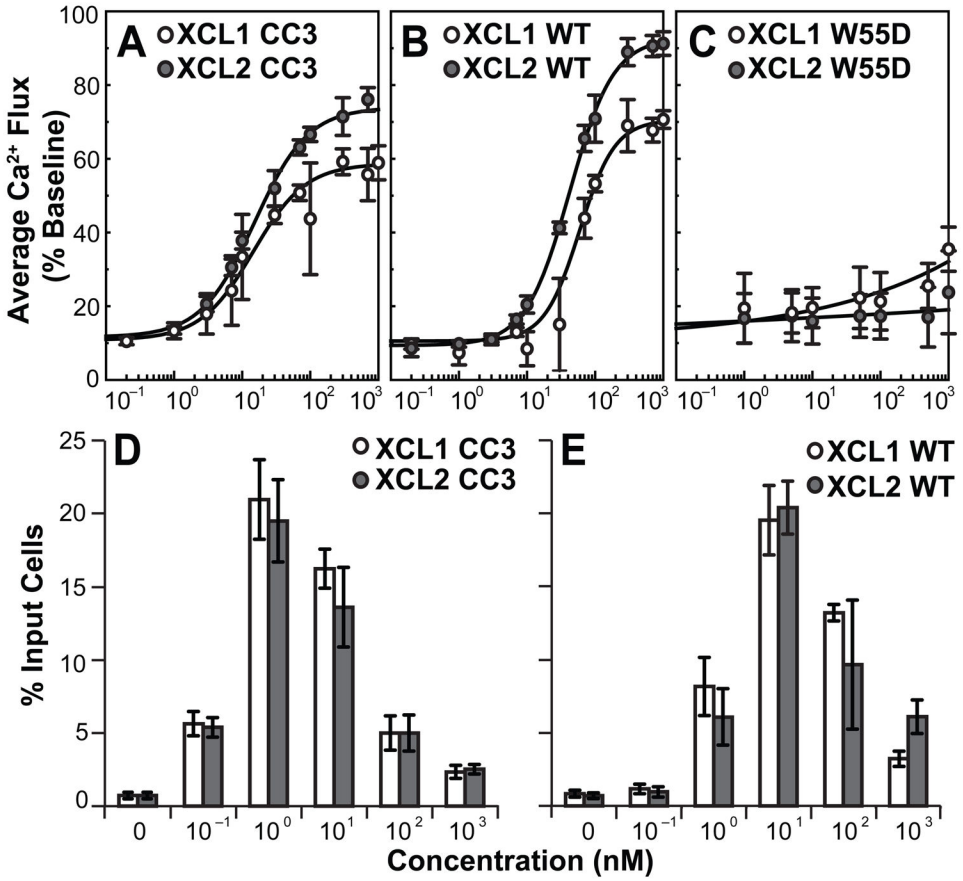

FIGURE 3. Ltn10 form of XCL2 activates XCR1

Ca^{2+} flux of HEK-293 XCR1 cells treated with various concentrations of XCL1/2 CC3 (A), XCL1/2 WT (B), and XCL1/2 W55D (C) in a concentration response experiment. Calculated EC_{50} values were: EC_{50} (XCL1 CC3) = 14.5 ± 3.6 nM, EC_{50} (XCL2 CC3) = 15.2 ± 2.4 nM, EC_{50} (XCL1 WT) 59.2 ± 7.4 nM, and EC_{50} (XCL2 WT) = 42.3 ± 3.3 nM. EC_{50} values were not measurable for the W55D variants. Chemotaxis response of murine L1.2 cells transfected with human XCR1 were treated with XCL1/2 CC3 (D), and XCL1/2 WT (E). Untransfected L1.2 cells were subjected to the same protein treatment as a negative control (not shown).

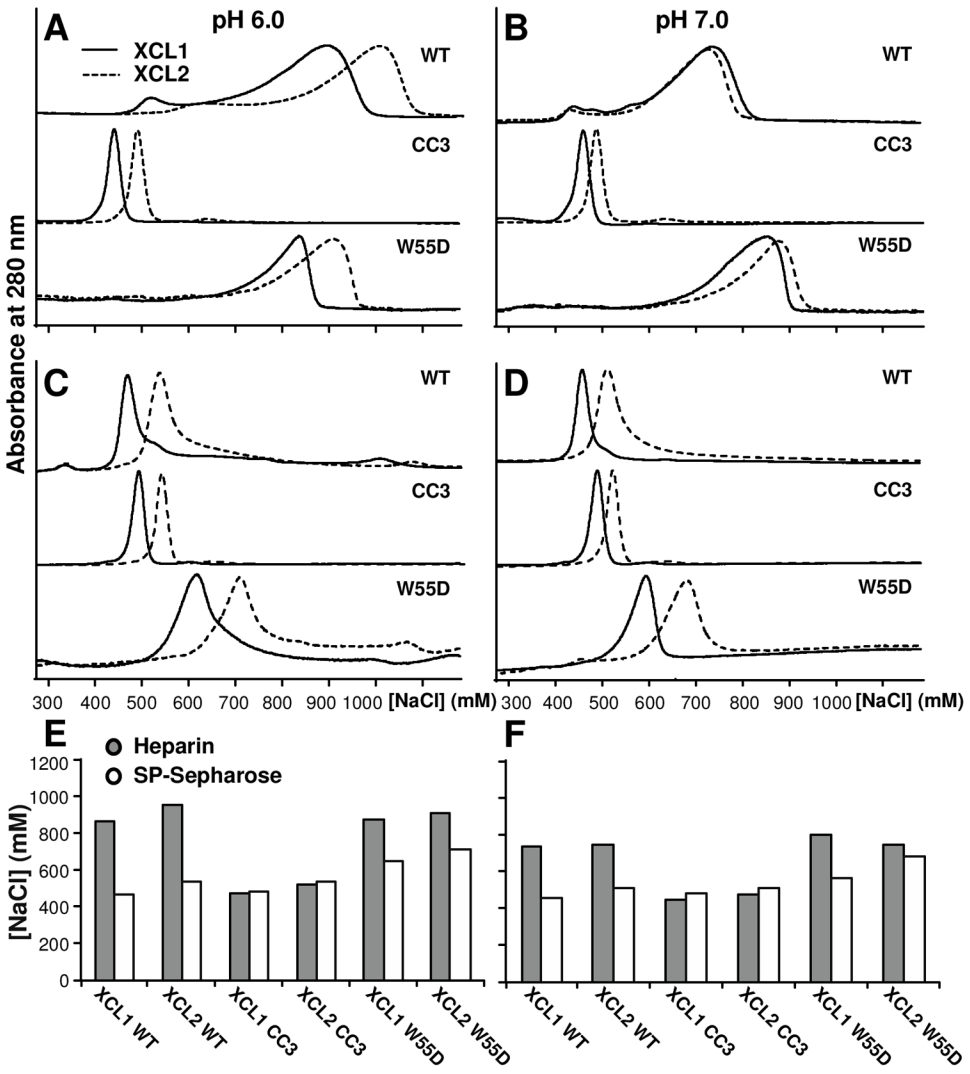

FIGURE 4. Ltn40 is responsible for heparin binding

Analysis of recombinant protein elution from heparin sepharose and cation exchange SP-sepharose as a function of increasing NaCl gradient. W55D is an engineered variant of XCL1 and XCL2 that is selective for the Ltn40 conformation. A) Elution of proteins from heparin column at pH 6.0. B) Elution from heparin at pH 7.0. C) Elution from SP-sepharose at pH 6.0. D) Elution from SP-sepharose at pH 7.0. E) Bar graph comparing elution profiles from A & C. F) Bar graph comparing elution profiles from B & D.

Table 1

Calculating the specificity of XCL1- and XCL2-heparin interactions from heparin and cation exchange chromatography.

	[1] Protein	[2] Heparin [NaCl] (mM)	[3] Δ [NaCl]^H (mM)	[4] S-Seph [NaCl] (mM)	[5] Δ [NaCl]^S (mM)	[6] $\Delta\Delta$ [NaCl] (mM)
pH 6.0	XCL1 WT	900	-	470	-	-
	XCL2 WT	1010	−110	540	−70	−40
	XCL1 CC3	440	460	500	−30	490
	XCL2 CC3	490	410	540	−70	480
	XCL1 W55D	830	70	620	−150	220
	XCL2 W55D	910	−10	710	−240	230
pH 7.0	XCL1 WT	730	-	460	-	-
	XCL2 WT	720	10	510	−50	60
	XCL1 CC3	460	270	490	−30	300
	XCL2 CC3	490	240	520	−60	300
	XCL1 W55D	850	−120	600	−140	20
	XCL2 W55D	900	−170	680	−220	50

[1] Recombinant XCL1 and XCL2 proteins were eluted from heparin sepharose and SP-sepharose columns at pH 6.0 (top panel) and pH 7.0 (bottom panel) as previously described.

[2,4] The elution peak for each protein was recorded as a function of NaCl concentration.

[3] $\Delta[NaCl]^H$ and

[5] $\Delta[NaCl]^S$ were calculated by subtracting heparin and SP-sepharose elution values from XCL1 WT.

[6] $\Delta\Delta[NaCl] = \Delta[NaCl]^H - \Delta[NaCl]^S$. By subtracting the electrostatic contribution, from the protein-heparin interaction, we are able to determine the relative affinity of each protein for heparin. The smaller values of $\Delta\Delta[NaCl]$ are indicative of specific heparin-binding affinity.

Table 2

Thermodynamic and kinetic parameters of XCL1 and XCL2 WT.

	Protein	k_{fwd}	k_{rev}	k_{fwd}/k_{rev}	K_{eq}
−NaCl	**XCL1 WT**	0.2 ± 0.1	0.7 ± 0.1	0.3 ± 0.2	1.7 ± 0.7
	XCL2 WT	0.2 ± 0.1	1.1 ± 0.3	0.2 ± 0.1	5.9 ± 4.2
+NaCl	**XCL1 WT**	0.4 ± 0.1	0.3 ± 0.1	1.3 ± 0.5	0.6 ± 0.5
	XCL2 WT	0.2 ± 0.1	0.3 ± 0.1	0.6 ± 0.4	2.2 ± 1.7